Electronic Supplementary Material (ESI) for RSC Advances.

Supporting Information

Combustion deposition of MoO_3 films: from fundamentals to OPV applications

Wouter Marchal[1], Christopher De Dobbelaere[1], Jurgen Kesters[2], Gilles Bonneux[1], Joke Vandenbergh[2], Hanne Damm[1], Tanja Junkers[2,3], Wouter Maes[2,3], Jan D'Haen[3,4], Marlies K. Van Bael[1,3], An Hardy[1,3]

1. Hasselt University, Institute for Materials Research, Inorganic and Physical chemistry, Martelarenlaan 42, 3500 Hasselt, Belgium

2. Hasselt University, Institute for Materials Research, Organic and Bio-polymer chemistry, Martelarenlaan 42, 3500 Hasselt, Belgium

3. IMEC vzw, division IMOMEC, Agoralaan Building D, 3590 Diepenbeek, Belgium

4. Hasselt University, Institute for Materials Research, Materials Physics, Martelarenlaan 42, 3500 Hasselt, Belgium

This Supporting information section includes 15 sections, labeled from S1 to S15, including both figures and tables.

Figure S1. Cross section SEM image of MoO_x film deposited on a Si/SiO_2 native oxide substrate processed with the same spin coat parameters as the studied films in TG-MS. The films were subjected to a temperature of 200°C in ambient atmosphere.

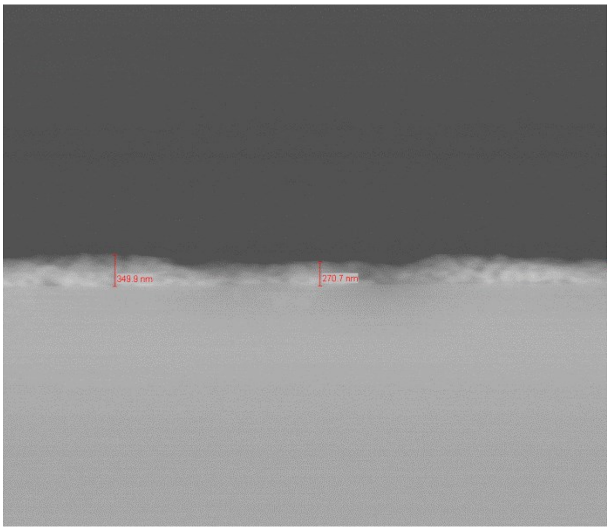

Figure S2. ESI-MS assignment of molybdenum-containing species with a single Mo-nucleus.

Signal 176.91			
Mo nucleus	calculated MW	experimental MW	Mo abundance
^{92}Mo	170.9098	170.9099	14.77%
^{94}Mo	172.9081	172.9083	9.23%
^{95}Mo	173.9088	173.9094	15.91%
^{96}Mo	174.9076	174.9079	16.68%
^{97}Mo	175.9090	175.9089	9.56%
^{98}Mo	176.9084	176.9069	24.19%
Signal 244.94			
^{92}Mo	238.9437	238.9358	14.77%
^{94}Mo	240.9420	240.9343	9.23%
^{95}Mo	241.9427	241.9158	15.91%
^{96}Mo	242.9415	242.9336	16.68%
^{97}Mo	243.9429	243.9405	9.56%
^{98}Mo	244.9423	244.9348	24.19%

ESI assignment of the molybdenum-containing species with two Mo-nuclei. Because of the large amount of possible combinations of Mo-isotopes (resulting in a complicated ESI-MS pattern), only the mass of the species containing two ^{98}Mo nuclei is calculated below.

theoretical m/z	experimental m/z
322.7985	322.8048
369.7778	369.8443

Figure S3. TGA and DTA of dried molybdenum precursor powders [ox/fuel] = 1, heating rate: 10 °C/min, powder fraction > 1 mm, in dry air and N_2 atmosphere, sample mass air = 3.179 mg, sample mass N_2 = 3.5680 mg.

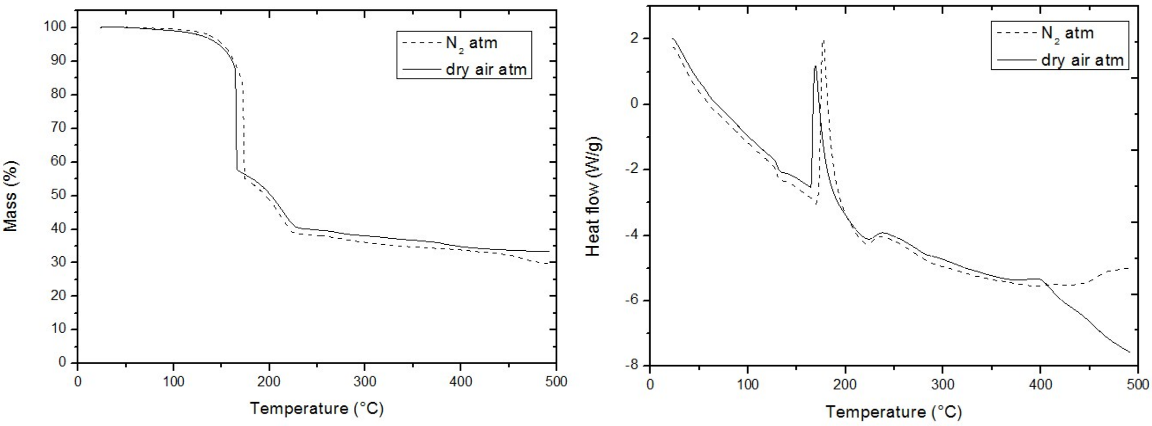

Figure S4. TGA of dried Molybdenum precursor powders [ox/fuel] = 1, heating rate 10 °C/min, powder fraction < 63 µm, in dry air as a function of pre-TGA drying temperature. Results indicate increased residual mass at higher drying temperatures.

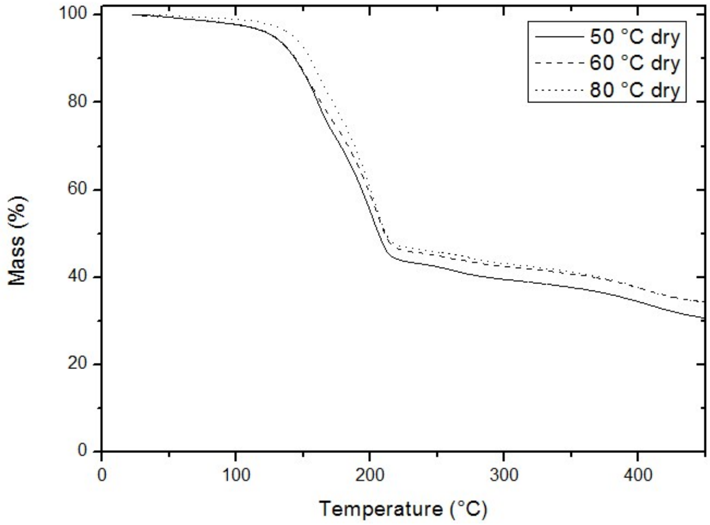

Figure S5. Corresponding FTIR spectra of precursor powders dried at temperatures in the range between 50 °C and 80 °C (mixture of $MoO_2(acac)_2$ and NH_4NO_3 from methanol precursor solution) on the left hand side, showing no decomposition of the organic components or influence of hydrolysis. Absorption in > 3000 cm^{-1} region is attributed to the NH_4NO_3 (FTIR spectrum at right hand side).

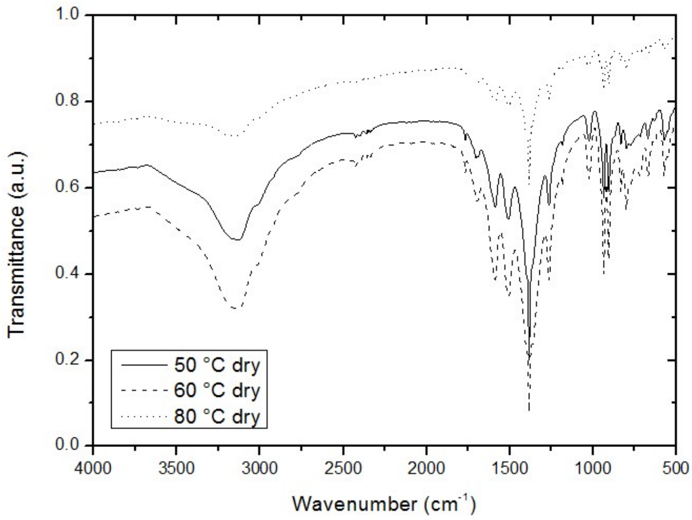

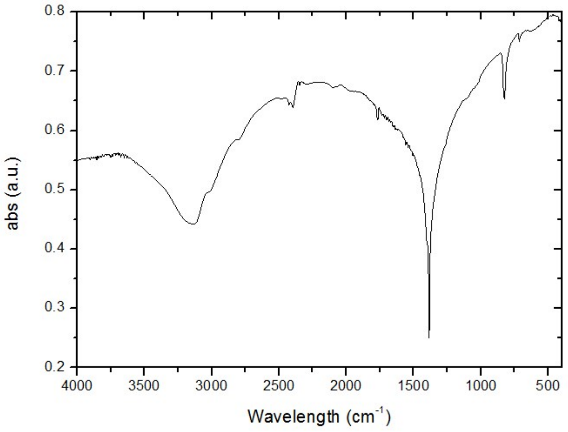

Figure S6. TG-FTIR images of the evolved components above 250 °C, [ox/fuel] = 1, heating rate: 10 °C/min. Spectra below indicate NH_3 and H_2O evolution at 285 °C, and CO_2 and H_2O evolution at 385 °C. The signals indicate a more significant CO_2 evolution for the 63 µm size fraction which can be related to the TGA results above.

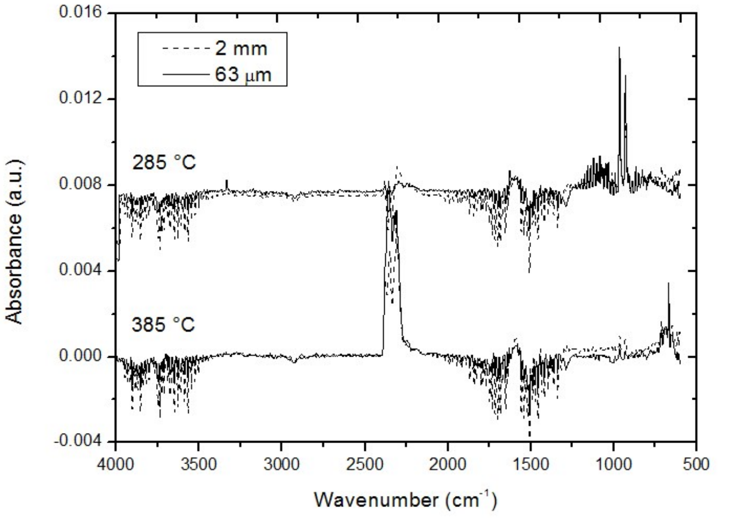

Figure S7. Cross section SEM images of MoO_3 layers. The shown images are recorded after deposition of respectively 4 and 8 layers by spin coating. From these results, the approximate thickness per layer can be calculated.

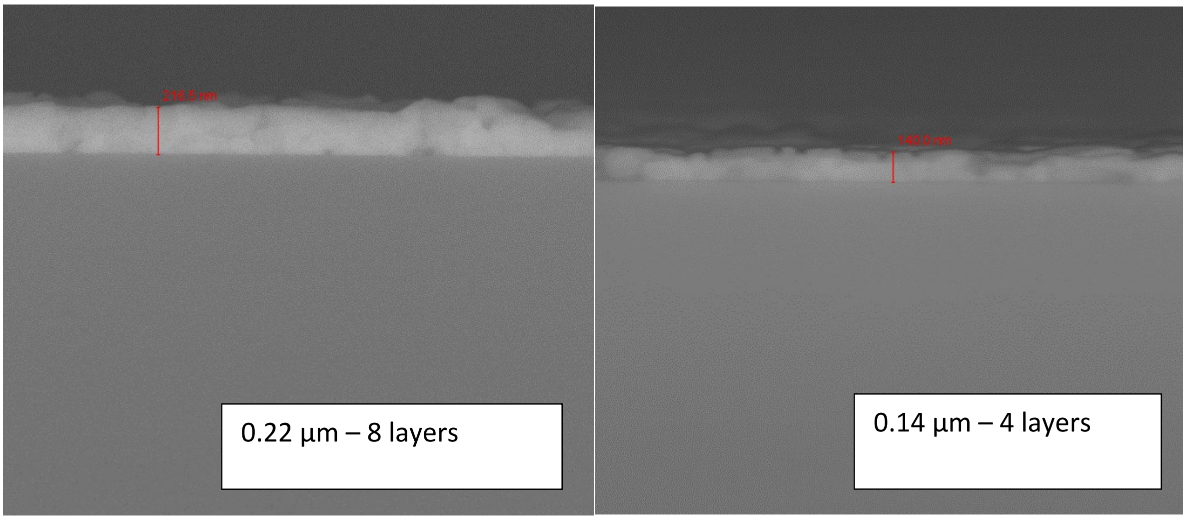

Figure S8. Reproducibility of TGA measurements, [ox/fuel] = 1, heating rate 10 °C/min, dry air atmosphere, pre-TGA drying at 80 °C

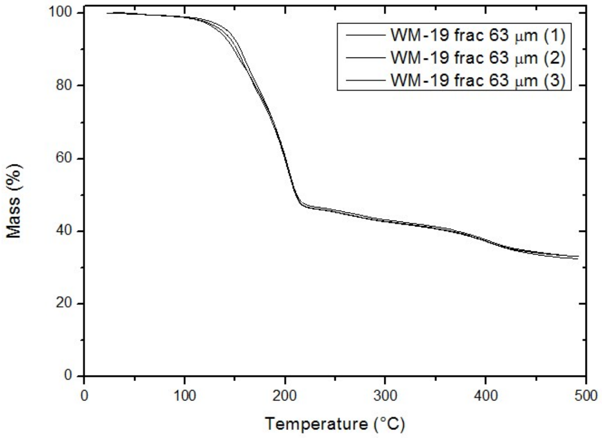

Figure S9. TGA (and DTA) results showing the removal of residual organics above 400 °C, indicating a more efficient removal of organics in case of a pronounced combustion reaction (decreased mass loss after 400 °C for 2 mm fraction). Dry air, 10 °C/min, drying at 60 °C, alumina sample pan.

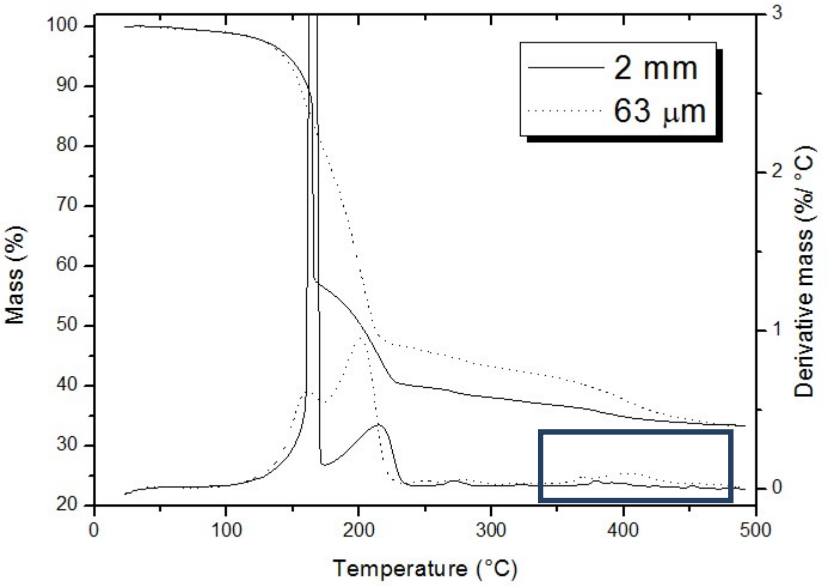

Figure S10. Overview of EGA from TG-FTIR of [ox/fuel] = 0.5. The 2 mm fraction single mass loss step corresponds to the right side spectrum (see Gram-Schmidt). The 63 µm fraction shows a more gradual mass loss and thereby an broad Gram-Schmidt signal. Therefore the FTIR spectrum is shown at two different temperatures to present a complete representation of the evolved components during the main mass loss step.

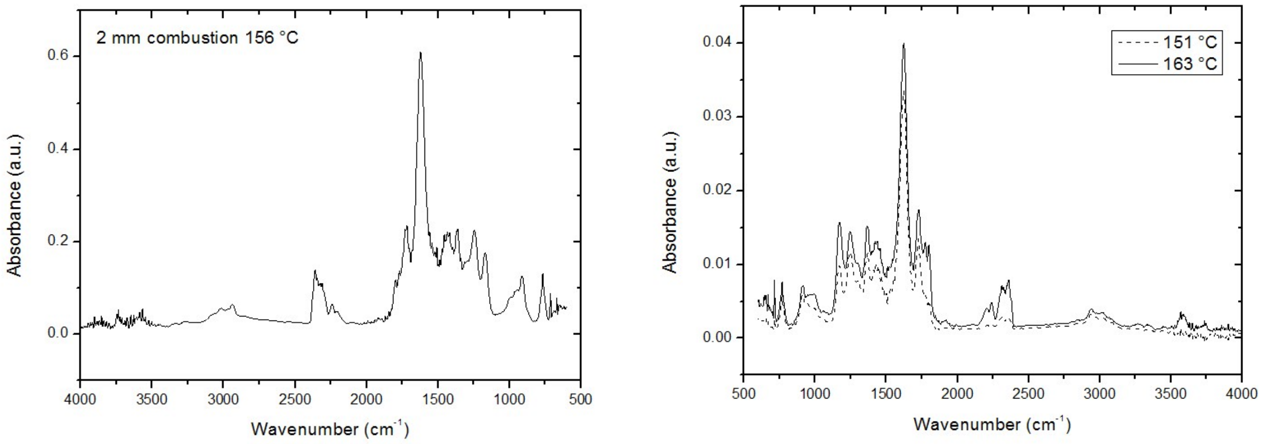

Again, the small size fraction shows an increased CO_2 signal which is conform aforementioned data of the [ox/fuel]= 1 precursor.

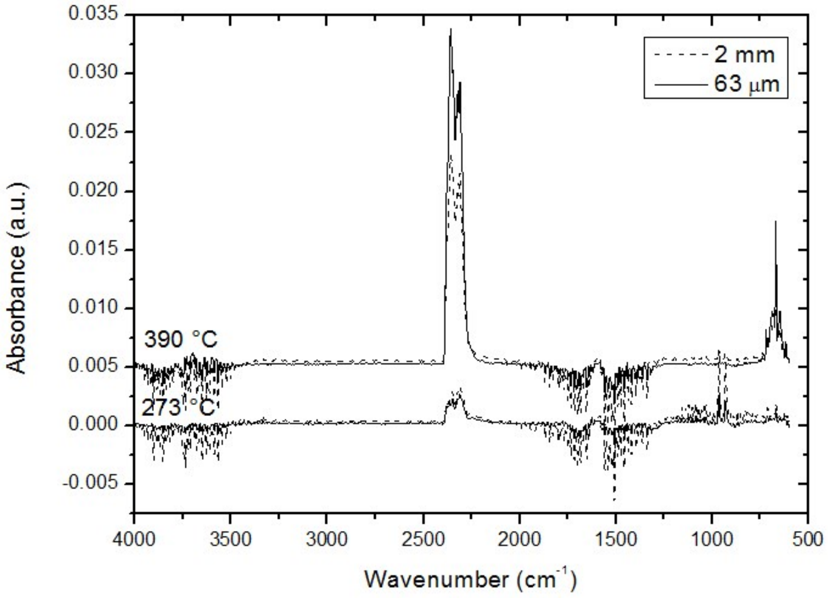

Figure S11. XRD diffractograms of MoO_x layers on ITO with different temperature treatment focusing on various heating rates (10 °C/min versus temperature jump 80 – 225 °C), and final annealing temperature of 225 °C for both samples. The most intensive signals indicating a crystalline MoO_x phase are located at 19.348°, 25.689 ° and 29.287°. These signals are clearly present in case of a temperature jump, whereas they are absent for the more gradually heated layer.

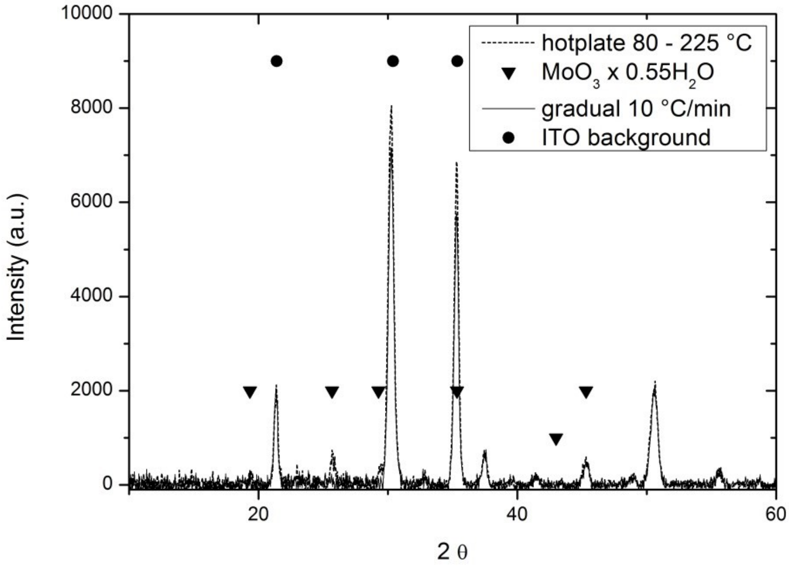

Figure S12: GATR-FTIR spectrum of MoO_3 layer after post-calcination in dry air on ITO substrate.

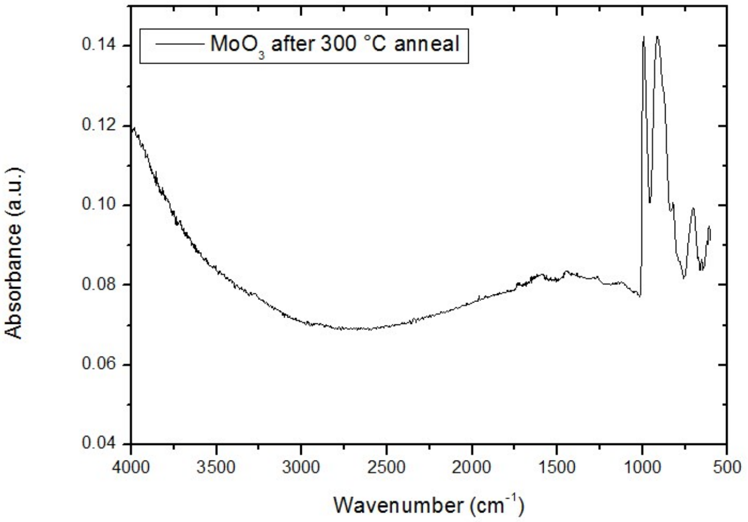

Figure S13. Detailed top down SEM image of the MoO_3 layer deposited from the 0.05 M precursor.

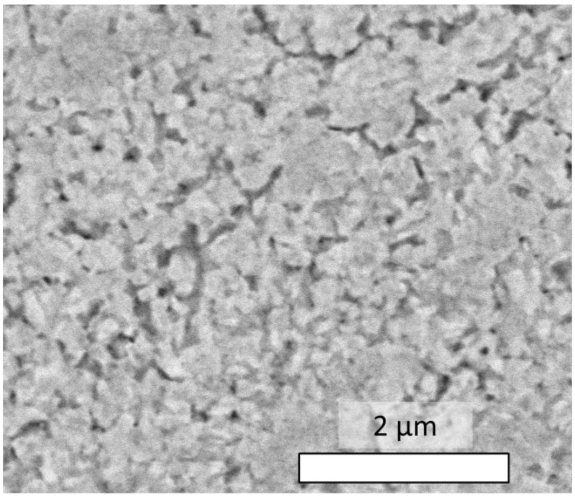

Figure S14. Tauc plots of a MoO_3 layer on ITO/borosilicate glass, background corrected, obtained after 4 subsequent layer depositions from the 0.1 M molybdenum precursor. The UV-vis spectrum is measured using the Cary 5000 spectrometer as described in the experimental section. Band gap fits were made for both the direct and indirect band gap. Both $(\alpha.h.\nu)^{1/2}$ and $(\alpha.h.\nu)^2$ are plotted on the ordinate to give an estimate of both the indirect and direct band gap respectively.

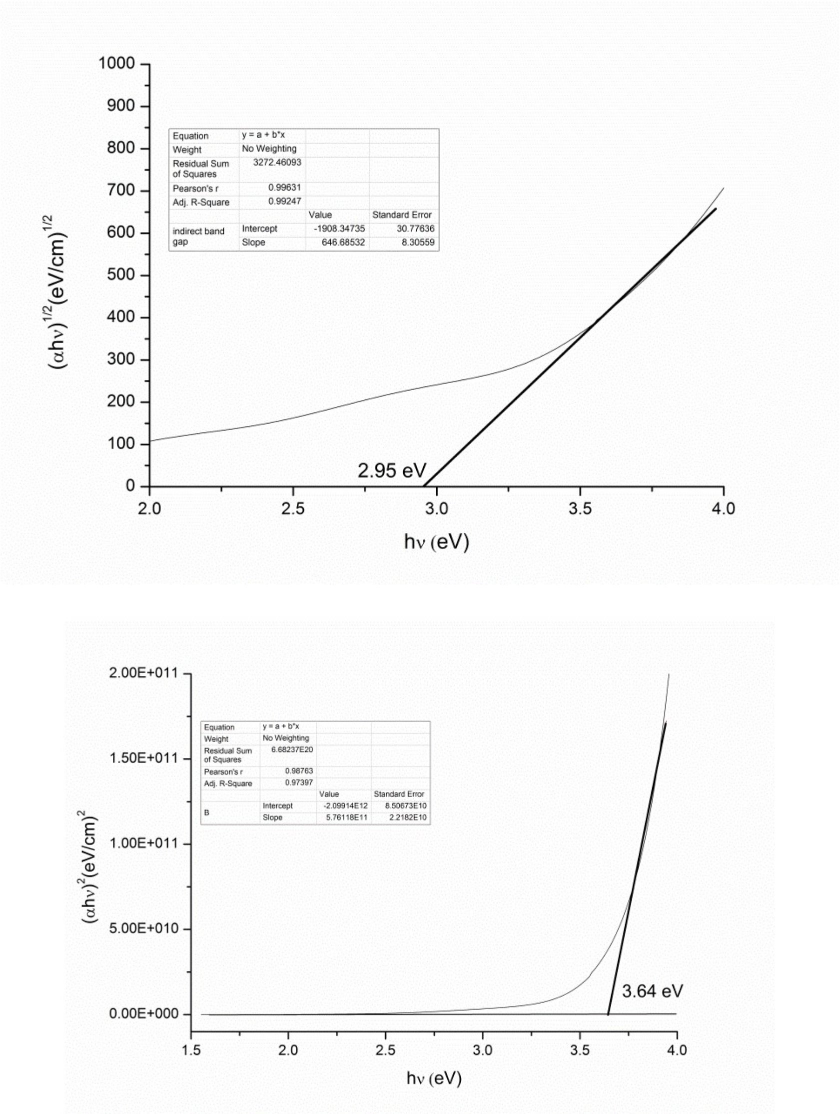

Equation	y = a + b*x		
Weight	No Weighting		
Residual Sum of Squares	3272.46093		
Pearson's r	0.99631		
Adj. R-Square	0.99247		
		Value	Standard Error
indirect band gap	Intercept	-1908.34735	30.77636
	Slope	646.68532	8.30559

Equation	y = a + b*x		
Weight	No Weighting		
Residual Sum of Squares	6.68237E20		
Pearson's r	0.98763		
Adj. R-Square	0.97397		
		Value	Standard Error
B	Intercept	-2.09914E12	8.50673E10
	Slope	5.76118E11	2.2182E10

Figure S15. Raman measurement comparing different hotplate treatments affecting the substrate heating rate.

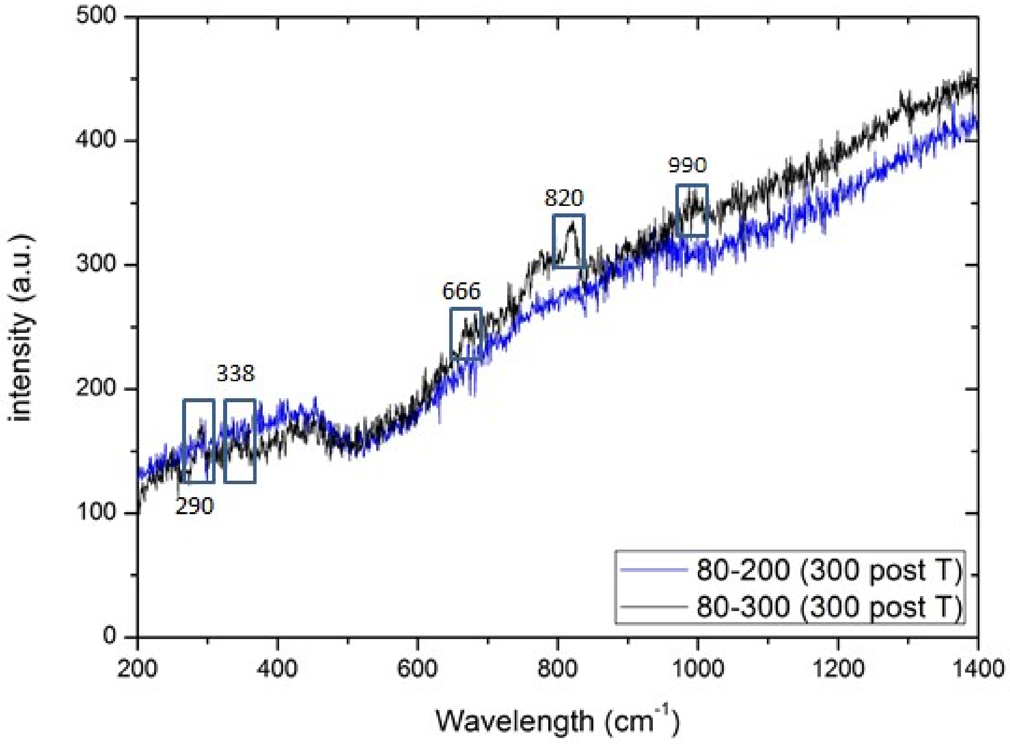
intensity (a.u.)
Wavelength (cm^{-1})
0
100
200
300
400
500
200
400
600
800
1000
1200
1400
290
338
666
820
990
80-200 (300 post T)
80-300 (300 post T)